Structural, Chemical, and Electronic Properties of Cu/Ta(110)

W. Kevin Kuhn,[†] Robert A. Campbell,[‡] and D. Wayne Goodman[*]

Department of Chemistry, Texas A&M University, College Station, Texas 77843

Received: June 8, 1992; In Final Form: September 8, 1992

The properties of ultrathin Cu films on a Ta(110) substrate have been studied using X-ray photoelectron spectroscopy (XPS), low-energy electron diffraction (LEED), temperature-programmed desorption (TPD), and infrared reflection adsorption spectroscopy (IRAS). For coverages of <1.2 monolayer the Cu overlayers grow pseudomorphic with respect to the Ta substrate. XPS results indicate that the Cu($2p_{3/2}$) binding energy of the supported Cu atoms is perturbed by +0.3 eV compared to that of the surface atoms in Cu(100). These electronic and physical perturbations induce distinct differences in the chemisorptive properties of the Cu films. This is evidenced by CO TPD results which indicate a 50 K increase in the CO desorption temperature as well as a CO stretching frequency that is 20 cm^{-1} higher than observed for the Cu(111) surface. A comparison of these results with those previously obtained for Cu overlayers on different substrates shows a correlation among the electronic perturbations of the adlayers, the metal-substrate bond strengths, the CO desorption temperatures, and the C-O stretching frequencies.

I. Introduction

The study of the structural, chemical, and electronic properties of ultrathin metal films supported on single-crystal metal substrates is an active area of research.[1-3] Since Cu is a component in several important bimetallic catalysts, Cu overlayers have been studied on a variety of substrates.[4-23] A major goal in these studies of model bimetallic systems has been the determination of how the changes in physical and electronic structure change the chemical properties of the overlayer, i.e., the catalyst. Once determined, the trends observed could lead to the design of catalysts with specific properties.

Temperature-programmed desorption (TPD) results for Cu on Re(0001),[15] Ru(0001),[6] Mo(110),[19] and Rh(100)[10] show two discrete features corresponding to Cu desorption from monolayer and multilayer states. For Cu on Pt(111), on the other hand, only one Cu desorption feature is observed and is attributed to the formation of a Cu-Pt alloy.[17] Studies of CO chemisorption have shown that the CO desorption temperatures from monolayer Cu on Re(0001), Ru(0001), Rh(100), and Pt(111) are 205,[15] 210,[4] 240,[11] and 250 K,[17] respectively. These temperatures are higher than is observed for CO desorption from Cu(111) or Cu(100) (185 K).[25] In addition to TPD, Auger electron spectroscopy (AES), X-ray photoelectron spectroscopy (XPS), infrared reflection-absorption spectroscopy (IRAS), and low-energy electron diffraction (LEED) have been used to characterize the ultrathin Cu layers on these substrates.[4-24] These studies have shown that at 100 K Cu typically forms a stable bilayer, with additional layers being metastable, coalescing into 3-D islands upon annealing to ~600-900 K.[4,24]

The results of our recent study of ultrathin Cu films on the Ta(110) substrate will be presented and discussed in this paper. The structural, chemical, and electronic properties of the Cu/Ta(110) system will be compared to previously studied Cu overlayer systems, and the results will be analyzed for observable trends in the Cu-substrate bond strengths, electronic perturbations, and CO desorption temperatures.

* To whom correspondence should be addressed.
†Present address: Frank J. Seiler Research Labs, USAF Academy, CO 80840.
‡Present address: Department of Physics and Astronomy and Lab for Surface Modification, Rutgers, The State University of New Jersey, Piscataway, NJ 08855-0849.

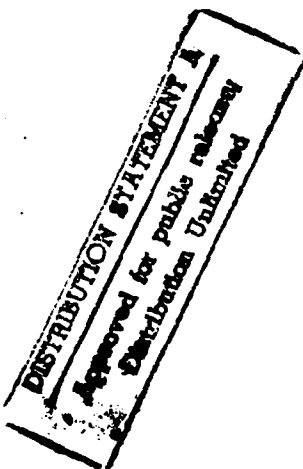## II. Experimental Section

The experiments were performed in two separate ultrahigh-vacuum (UHV) chambers. The first system (base pressure ≤5 × 10^{-10} Torr) was equipped for AES, XPS, LEED, and TPD measurements and has been described in detail elsewhere.[26] The second system (base pressure ≤2 × 10^{-10} Torr) was equipped for IRAS, AES, LEED, and TPD and has been described in detail elsewhere.[27] The IRAS spectra were acquired for 256 scans in the single reflection mode at a resolution of 4 cm^{-1} and an incidence angle of 85° off the surface normal.

The Ta(110) crystal was attached to the manipulator by two Ta support leads, and the sample temperature was monitored by a W/5%Re-W/26%Re thermocouple spot-welded to the sample edge. The manipulator allowed resistive heating to 1600 K and liquid nitrogen cooling to 100 K. An electron beam assembly allowed heating to 2400 K. The surface was cleaned by successive annealing cycles to 2400 K. The cleanliness and long-range order were verified with AES, XPS, and LEED.

Cu was deposited onto the crystal surface via evaporation from a resistively heated W wire wrapped with high-purity Cu wire. To ensure film cleanliness, the surfaces were flashed to 500 K after metal deposition (unless stated otherwise) to remove possible contaminants, after which no contaminants were detectable by XPS or AES. All adsorbate coverages are referenced with respect to the number of Ta surface atoms (1.30 × 10^{15} atoms/cm^2) with one Cu atom per Ta atom corresponding to θ_{Cu} = 1.00 monolayer (ML). Linear heating rates of 5 and 10 K/s were used in the CO and Cu desorption measurements, respectively.

The Cu($2p$) and Ta($4f$) XPS spectra were acquired using an Al Kα X-ray source and a hemispherical energy analyzer. The Cu($2p_{3/2}$) binding energies were referenced to the Ta($4f$) peak with an experimental error of 0.03 eV. Detection was normal to the surface in XPS and AES.

III. Results

The thermal desorption spectra of Cu overlayers from Ta(110) are shown in Figure 1. For submonolayer Cu coverages, only one desorption feature is present, with the desorption temperature of these films shifting toward higher temperature as the Cu coverage is increased. For 1 ML of Cu, the desorption temperature is found to be 1265 K. For Cu coverages greater than 1 ML, two features are present, with the new desorption peak occurring at a lower temperature than for the monolayer peak. The fact that
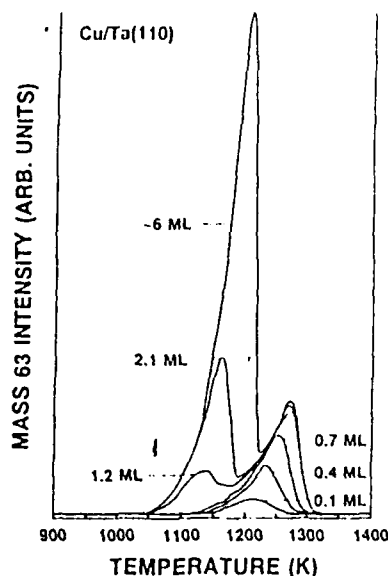
Figure 1. Thermal desorption spectra for Cu films on Ta(110). The Cu films were vapor-deposited at ~350 K and annealed to 500 K prior to TPD acquisition.

there are two peaks present in the Cu TPD indicates that Cu is forming multiple layers on the Ta(110) surface; that is, Cu and Ta do not form an alloy. This is supported by the solid-state Cu–Ta phase diagram which indicates that, at the concentrations and temperatures used in this study, Cu and Ta are immiscible. The low-temperature multilayer peak shifts toward higher temperature as the Cu coverage is further increased, and the traces for his peak exhibit a common leading edge typical of the zero-order desorption kinetics observed for copper overlayers.[5,11,15,20,21] Leading edge analysis of the Cu/Ta(110) desorption data yields a desorption activation energy of ~73 kcal/mol for the multilayer desorption state. This value of 73 kcal/mol for multilayer Cu compares well with the bulk sublimation energy of Cu (~76 kcal/mol [28]). The Cu desorption features arising from monolayer and submonolayer Cu films, however, have neither the common leading edges and sharp high-temperature tails characteristic of zero-order desorption nor the common peak desorption temperature characteristic of first-order desorption. Therefore, the desorption kinetics are likely fractional order. A Redhead analysis of the monolayer desorption peak (which is at a constant temperature for 1–6 ML Cu films) yields a desorption activation energy of ~79 kcal/mol.

Ordering of the Cu overlayers is evident from LEED observations. Figure 2 shows typical LEED patterns observed for different overlayer coverages at ~100 K. For submonolayer films annealed to 900 K, the pattern observed (Figure 2b) is a diffuse (1 × 1) pattern indicating that the Cu adatoms are forming small pseudomorphic islands. For Cu coverages greater than ~1.5 ML that were annealed to 900 K, a (9 × 2) pattern is observed (Figure 2c). A schematic illustration of the (9 × 2) LEED pattern is shown in Figure 2d. The multiple diffraction spots along the (1$\bar{1}$0) crystal axis indicate a lattice mismatch along this axis with the Cu overlayer compressing along this axis to assume lattice dimensions that are closer to those of Cu(111). LEED observations for unannealed Cu monolayers show only diffuse (1 × 1) patterns with relatively high background intensity.

Figure 3 shows XPS spectra of the Cu(2p$_{3/2}$) peak for different Cu overlayer thicknesses. To ensure surface cleanliness, after the Cu was deposited onto the Ta(110) substrate at ~350 K, the sample was annealed to 500 K to remove any adsorbed CO prior to spectral acquisition. Adlayers with a thickness of less than or equal to 1 ML show a constant peak position of 933.03 eV which shifts to 932.90 eV as the Cu coverage is increased. This peak shift is shown more clearly in Figure 4a where the value for the

peak centroid is plotted with respect to the Cu coverage as determined via TPD measurements. For coverages greater than 1 ML, the XPS spectra represent a combination of electrons being emitted from surface and subsurface Cu atoms. Previous experiments on Cu(100) have shown that there is a 0.22-eV shift to lower binding energy for the surface Cu atoms compared to bulk copper.[29] Figure 4b compares the 0.17-eV shift to lower binding energy of the surface layer of Cu atoms on a pure Cu sample to the 0.13-eV shift to higher binding energy of a monolayer of Cu on Ta(110). This indicates that the Cu monolayer on Cu/Ta(110) is shifted 0.30 eV toward higher binding energy compared to the surface layer of Cu in Cu(100).

CO TPD spectra from Cu/Ta(110) surfaces are shown in Figure 5. For CO adsorbed on a clean Ta(110) surface there were no CO desorption features for temperatures between 100 and 1500 K. For Figure 5a, the Cu was deposited onto the surface at 100 K prior to a saturation (20 langmuirs) CO exposure at 90 K. For submonolayer Cu coverages, as the Cu coverage increases, there is a corresponding decrease in CO desorption temperature. This likely reflects the deposition of the Cu overlayers as a random mixture of small 2-D and 3-D islands. Extrapolating the CO desorption temperatures to zero Cu coverage yields a temperature of ~275 K. This would be the expected desorption temperature of CO from individual Cu atoms on a Ta(110) surface. For Cu coverages of ≥0.9 ML, CO desorption occurs at 180 K, which is very similar to that observed for Cu(111).[25] This implies a predominance of 3-D Cu clusters on the surface. A possible explanation for this unusual 3-D cluster predominance at monolayer coverages is that the dissociated adsorption of CO on bare Ta domains leads to a buildup of atomic C and O which induces clustering of the Cu adatoms. Figure 5b shows the CO desorption spectra from Cu overlayers which were annealed to 900 K prior to receiving a saturation CO exposure at 90 K. At low Cu coverages, two peaks are present at ~230 and ~210 K (α_1 and α_2, respectively). For coverages greater than 1 ML, the α_1 peak persists with a new peak at ~180 K (α_3) growing in and eventually becoming dominant. The α_1 and α_3 states likely correspond to CO desorption from the pseudomorphic overlayer and 3-D clusters, respectively. The origin of the α_2 peak is uncertain but could correspond to CO desorption from the Cu/Ta interface between the substrate and 2-D or 3-D Cu islands. The fact that annealed submonolayer Cu films do not exhibit a predominance of 3-D Cu clusters implies that the CO that is dissociatively adsorbed on the bare Ta domains cannot induce clustering of the Cu to a significant degree.

Figure 6 illustrates the effects of CO adsorption on the Cu-(2p$_{3/2}$) binding energy region for monolayer and submonolayer coverages of Cu. The Cu was deposited at ~110 K and flashed to 500 K prior to a saturation CO exposure (20 langmuirs) at ~110 K. The formation of a CO–Cu bond shifts the Cu(2p$_{3/2}$) peak 0.30 eV toward higher binding energy at a Cu coverage of 1 ML. For low Cu coverages, the induced shift was even larger (~0.40 eV). These binding energy shifts were reversible. The binding energy observed after flashing to 500 K to desorb the CO was identical with the binding energy observed before CO adsorption.

IR spectra for CO adsorbed on different Cu coverages on the Ta(110) substrate are shown in Figure 7. In Figure 7a, Cu deposition, CO dosing, and spectral acquisition were all conducted at 90 K. In Figure 7b, the Cu was deposited at 90 K, annealed to 900 K, and then cooled to 90 K for the saturation CO exposure and spectral collection. CO adsorbed on Ta(110) gives a broad, weak feature at ~2100 cm^{-1} indicating that although CO does not desorb from Ta(110) at temperatures <1500 K, CO adsorption at 90 K is not entirely dissociative. The large width of the CO/Ta(110) IR peak suggests considerable inhomogeneity in the adsorbed CO. This could be due to the atomic C and O that are also present on the surface due to CO dissociation. In Figure 7a,
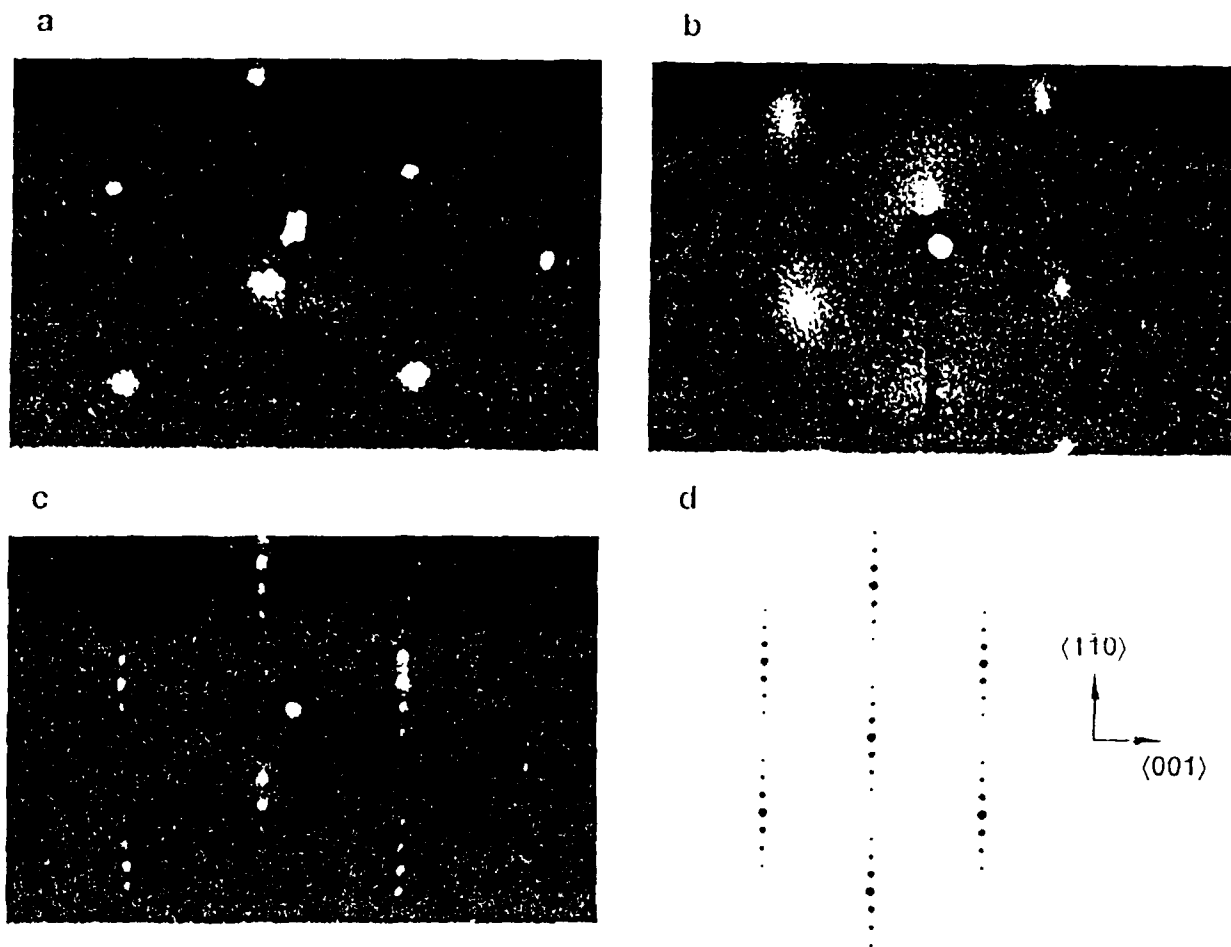
a

b

c

d

⟨1̄10⟩

⟨001⟩

Figure 2. LEED patterns associated with Cu deposition: (a) clean substrate (130 eV); (b) 0.65 ML, annealed to 900 K, diffuse (1 × 1) pattern (148 eV); (c) 1.8 ML, annealed to 900 K, (9 × 2) with multiple diffraction splitting along the (1̄10) axis; (d) a schematic illustration of the (9 × 2) pattern.
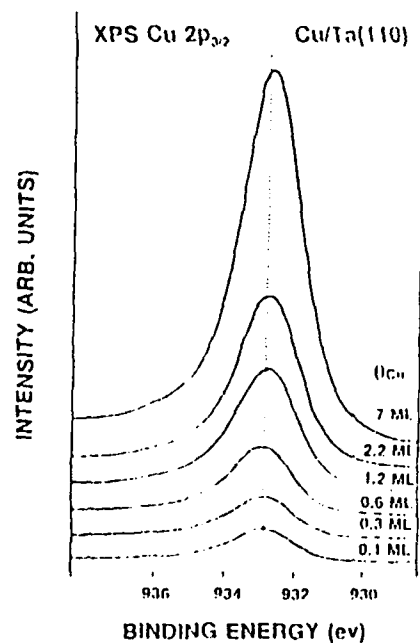
XPS Cu 2p₃/₂   Cu/Ta(110)

INTENSITY (ARB. UNITS)

0ᴄᵤ
7 ML
2.2 ML
1.2 ML
0.6 ML
0.3 ML
0.1 ML

936   934   932   930

BINDING ENERGY (ev)

Figure 3. Cu(2p₃/₂) XPS spectra of Cu/Ta(110) as a function of Cu coverage. The Cu films were vapor-deposited at ∼350 K and flashed to 500 K prior to spectral acquisition.

(a)   Cu/Ta(110)

933.10

933.00

Cu2p₃/₂ BINDING ENERGY (ev)

932.90

932.80

0   1   2   3   4   20

Cu COVERAGE (ML)

(b)   Cu (2p₃/₂) XPS

——— Cu(100) (surface + bulk)

0.17 eV

bulk Cu ——   —— surface layer in Cu(100)

0.22 eV

20 ML of Cu on Ta(110)

1 ML of Cu   0.13 eV on Ta(110)

0.30 eV

BINDING ENERGY

Figure 4. (a) Variation in Cu(2p₃/₂) binding energy as a function of coverage from spectra in Figure 3. (b) Relative binding energies of bulk Cu, the surface layer of Cu(100) atoms, and a monolayer of Cu on Ta(110).

it is noteworthy that, at a Cu coverage of 0.1 ML, the CO-Ta peak is no longer visible. This feature is apparently greatly attenuated by the CO-Cu overlayer as has been seen for other Cu overlayer systems.[9,11,18] In Figure 7b, the proximity of the CO-Ta and CO-Cu peaks makes it difficult to determine precisely
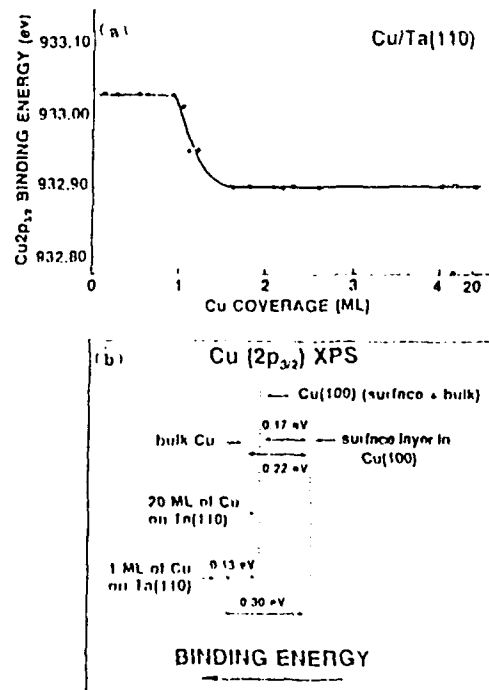
at what Cu coverage the CO-Ta peak is completely attenuated. The spectra for unannealed Cu overlayers in Figure 7a show a continuous red-shifting of the CO peak from ∼2123 to ∼2106
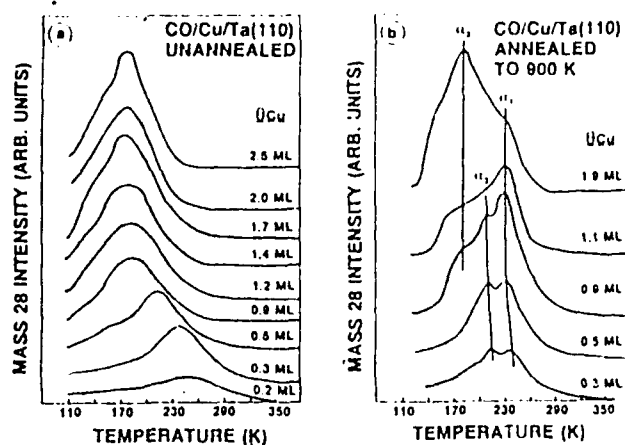
Figure 5. CO TPD from Cu/Ta(110) as a function of Cu coverage. The Cu was deposited at 100 K and either left unannealed (a) or annealed to 900 K (b) prior to a saturation CO (20 langmuirs) exposure at 100 K.
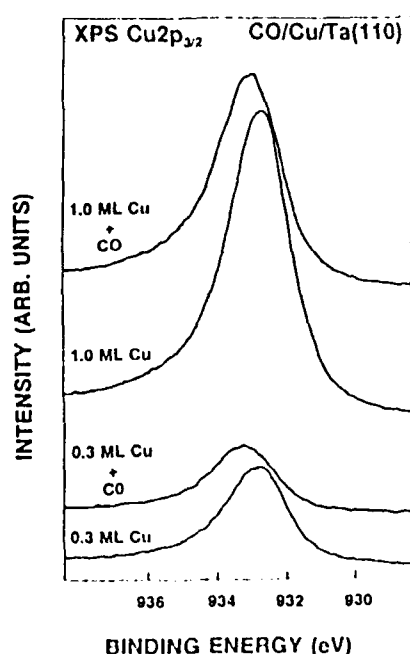

Figure 7. IR spectra of CO on Cu/Ta(110) as a function of Cu coverage. The Cu was vapor-deposited onto the surface at 100 K and either left unannealed (a) or annealed to 900 K (b) prior to saturation CO exposure and spectral acquisition at 90 K.

Figure 6. Effect of CO adsorption on the Cu(2p$_{3/2}$) spectra of Cu/Ta(110). The Cu was deposited at ~110 K and flashed to 500 K prior to a saturation (20 langmuirs) CO exposure at ~110 K.

Figure 8. IR spectra of CO on Cu/Ta(110) as a function of CO exposure: (a) 0.9 ML of Cu annealed to 900 K prior to CO exposure at 90 K· (b) 1.5 ML of Cu annealed to 900 K prior to CO exposure at 90 K.

cm^{-1} as the Cu coverage is increased from 0.1 to 2.0 ML, approaching the value observed for CO adsorbed on Cu(111) (~2070 cm^{-1}).[30] The 30-cm^{-1} difference is significant; however, the observed frequencies of ~2100-2110 cm^{-1} are similar to those seen for CO adsorption onto stepped Cu surfaces and supported Cu films.[31] In the annealed films shown in Figure 7b, on the other hand, the value of the CO peak is constant at 2095 cm^{-1} for Cu coverages between 0.3 and 0.9 ML. The constant frequency of this peak as the Cu coverage is increased suggests CO adsorption onto 2-D islands that are increasing in size via growth at the island edges. The CO IR peak shifts to 2102 cm^{-1} for CO on 1.5 ML of annealed Cu, reflecting the phase transition seen by LEED at this coverage. In addition, the annealed CO/Cu/Ta(110) peaks are, in general, narrower than the unannealed CO/Cu/Ta(110) peaks. This is attributed to the inhomogeneous broadening of the unannealed spectra due to the nonuniformity of these films.

Figure 8 shows the CO exposure dependence of the CO IR features for annealed Cu overlayers. In both parts a and b of Figure 8, the IR spectra show a shift to higher frequency which is typical of CO adsorption as the CO coverage is increased. It is, however, contrary to the slight shift to lower frequency that
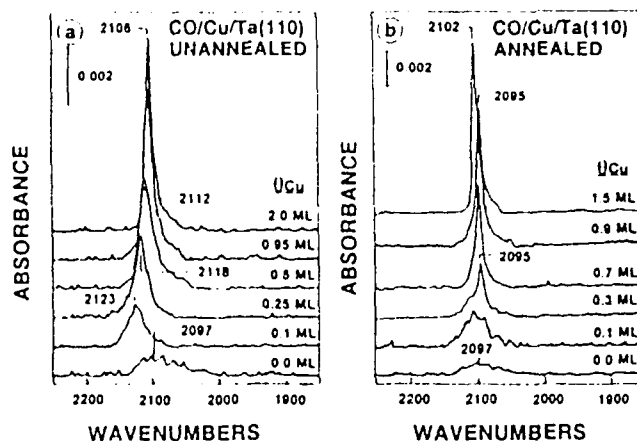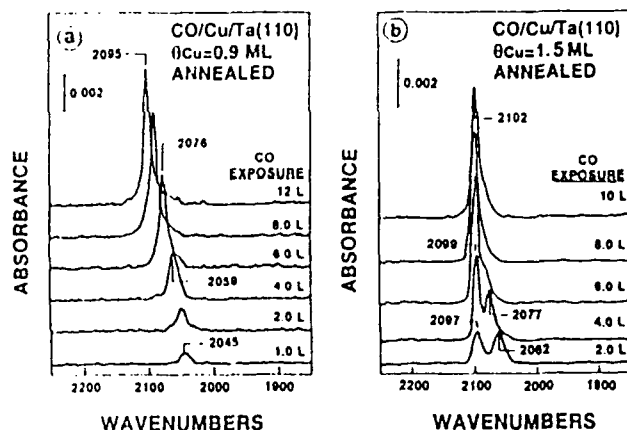
is observed for CO on Cu(111).[30] A coverage-dependent shift toward higher frequency with an increase in CO coverage has been observed previously for supported Cu monolayers[8,13] and different Cu crystal faces.[30a] The coverage-induced frequency shift is usually attributed to a decrease in back-donation as CO coverage increases or to an increase in dipole–dipole coupling.[32,33] An additional feature at a lower frequency is present in Figure 8b for low CO exposures. This low-frequency feature blue-shifts at a higher rate than the high-frequency peak and at saturation CO exposure is only visible as a slight shoulder on the main high-frequency peak (2102 cm^{-1}). Due to the proximity of the two peaks, there is likely a strong transfer of intensity from the low-frequency peak to the high-frequency peak.[34,35] As the CO coverage increases, this effect will increase due to the increased proximity of the CO molecules and the decrease in the separation between the peak frequencies. Thus, it is very likely, even at saturation CO coverage, that the low-frequency peak is the majority surface species.

IR spectra of CO on Cu/Ta(110) as a function of sample temperature are shown in Figures 9 and 10. For submonolayer Cu on Ta(110), Figure 9 shows a slight blue shift in the CO stretching frequency as the CO coverage decreases. In addition, the spectra in Figure 9, a and b, at ~0.1 and ~0.33 ML, respectively, show a decrease in the CO desorption temperatures as the Cu coverage is increased. In addition, Figure 10a ($\theta_{Cu} \simeq$ 1.8 ML) shows a desorption temperature of approximately 190 K. This decrease in desorption temperature as the copper coverage increases is in agreement with the TPD data shown in Figure 5a. Figure 10a,b again shows the effect of annealing the Cu overlayer
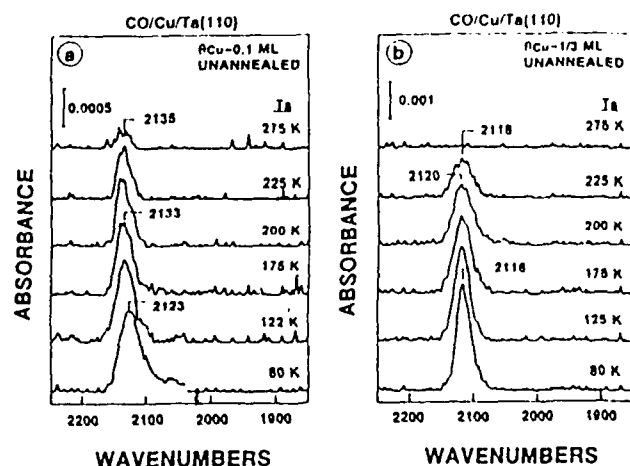
Figure 9. IR spectra of CO/Cu/Ta(110): 0.1 ML of Cu (a) or 0.33 ML of Cu (b) was deposited at 100 K with a subsequent saturation CO exposure at 90 K. The spectra were collected at the indicated temperatures.
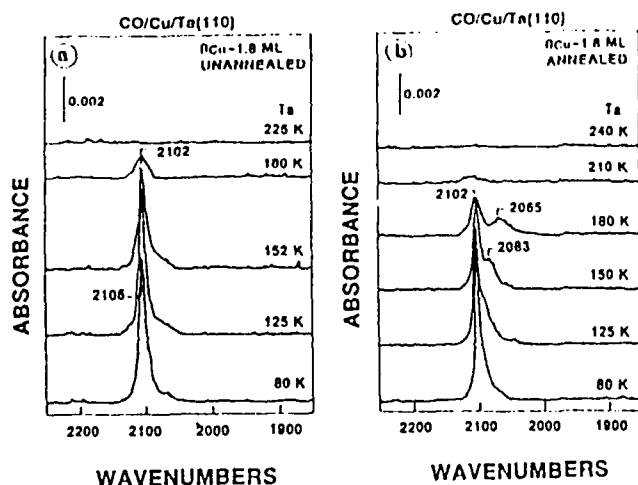

Figure 10. IR spectra of CO/Cu/Ta(110). Approximately 1.8 ML of Cu was deposited at 100 K and either left unannealed (a) or annealed to 900 K (b) prior to CO exposure at 90 K. The spectra were collected at the indicated temperatures.

prior to CO adsorption. In Figure 10b, the low-frequency shoulder that was present in Figure 8b for low CO exposures is present at elevated temperatures where the CO coverage is reduced. The CO peak in Figure 10a shifts slightly to lower frequency as the CO coverage decreases. This is in agreement with the exposure dependence observations shown in Figure 8a but is contrary to the shift seen in Figure 9 for submonolayer Cu films.

IV. Discussion

The results presented in the previous section indicate that, on a Ta(110) surface at 100 K, the Cu overlayer grows via the expansion and coalescence of small 2-D islands. In addition, before the first monolayer is completed, some of these 2-D islands nucleate into 3-D clusters. IR spectra of CO adsorbed on these clusters indicate that they are likely small due to the dominance of high-index adsorption sites. For annealed films, the first Cu layer grows pseudomorphically via the coalescence of small 2-D islands into a uniform monolayer with any additional Cu forming 3-D clusters. However, at a Cu coverage of ≥ 1.3 ML, annealing leads to the formation of a uniform overlayer that is more densely packed than the Ta(110) substrate. From the (9 × 2) LEED pattern observed, the overlayer is assigned a coverage of 1.22 ML for a uniform layer. Therefore, for coverages greater than 1.22 ML, the surface structure corresponds to a 1.22 ML (9 × 2) uniform layer with any additional Cu forming 3-D clusters on top of this uniform layer. A coverage of 1.22 ML corresponds to

1.59×10^{15} atoms/cm², which reflects the compression of the overlayer to a coverage that is closer to the surface atomic density of Cu(111) (1.77×10^{15} atoms/cm²). This coverage likely represents an equilibrium between two opposing forces on the Cu overlayer. One is the strain induced in the Cu overlayer by expanding the Cu(111) lattice to pseudomorphically fit the (110) surface of Ta. The other is the Cu–Ta bonding interaction, which is stronger than the Cu–Cu interaction for $\theta_{Cu} \leq 1.2$ ML, driving the Cu overlayer toward a pseudomorphic morphology. Thus, the 1.22 ML Cu overlayer density value represents a balance between the pseudomorphic 1.00 ML overlayer and a Cu(111) (1.36 ML equivalent) structure.

The (9 × 2) LEED pattern observed for Cu/Ta(110) is shown in Figure 2c and represents multiple diffraction of the electrons from the Cu overlayer. This phenomenon is not limited to Cu/Ta(110) but has been observed for several systems,[36–42] with the substrates typically being the (110) faces of bcc refractory metals. For the case of Cu/Ta(110), multiple diffraction was observed along the $(1\bar{1}0)$ crystal axis; however, for other systems, the splitting has been observed along the ⟨001⟩ and ⟨1$\bar{1}$0⟩ directions. In addition, for Cu/Mo(110) and Cu/W(110), splitting has been observed along both crystal axes with the orientation depending upon coverage and temperature.[36,37] For Cu/Nb(110), on the other hand, a LEED pattern indicative of Cu(100) was observed at submonolayer coverages with a Cu(111) type structure growing in at higher coverages.[42] Thus, it appears that the overlayer structure and axis along which the overlayer compression occurs depends not only upon coverage and annealing but also upon the specific substrate and its temperature.

The XPS results indicate that the atoms in a monolayer of Cu on Ta(110) have a higher Cu($2p_{3/2}$) binding energy than the surface atoms in Cu(100). This agrees with the results for Cu/Mo(110)[43] and Cu/Re(0001),[15,16] which also show shifts toward higher binding energy. These results indicate that electronic charge is transferred from the overlayer Cu atoms to the Ta, Mo, and Re substrate atoms upon bond formation. The removal of charge from a Cu atom to form a bond with the substrate increases the energy necessary to remove a core electron in the XPS measurement leading to the observed shift toward higher binding energy. Shifts in core level binding energies, however, must be regarded cautiously since changes in the screening of the core hole (final state effects) could give rise to the observed shifts. Several factors indicate that charge transfer is the primary source of the core level binding energy shifts. For example, the magnitude and direction of the charge transfer between overlayer and substrate atoms, observed with work function measurements,[21,40,44,45] support the UPS[23,46–48] and XPS[10,15,16,43] results. This correlation among work function, UPS, and XPS measurements implies that charge transfer is indeed the operative mechanism leading to the observed XPS binding energy shifts.

These charge-transfer effects have been discussed in detail previously in terms of a model where the different metals are designated as being electron rich or electron poor.[15,43,49] Metals on the left-hand side of the transition series, which are deficient in d electrons (e.g., Ta, W, etc.), are designated as electron poor whereas metals on the right-hand side, which have a more than half-filled d band (e.g., Pd, Pt, etc.), are designated as being electron rich. Upon bond formation charge transfer occurs from the electron-rich metal to the electron-poor metal. For Cu, the interactions can be explained by using the $3d^{10}4s^1$ electronic configuration to designate Cu as having a half-filled valence band. When a Cu monolayer is deposited onto an electron-rich substrate, e.g., Ru(0001), Rh(100), or Pt(111), for example, the Cu($2p_{3/2}$) binding energy will shift toward lower energy,[10,17] as can be seen in Figure 11a. Likewise, when Cu is deposited onto a substrate that has a less than half-occupied valence band (electron poor relative to Cu), charge transfer will occur from Cu to the substrate. These trends are clearly reflected in Figure 11a for Cu films
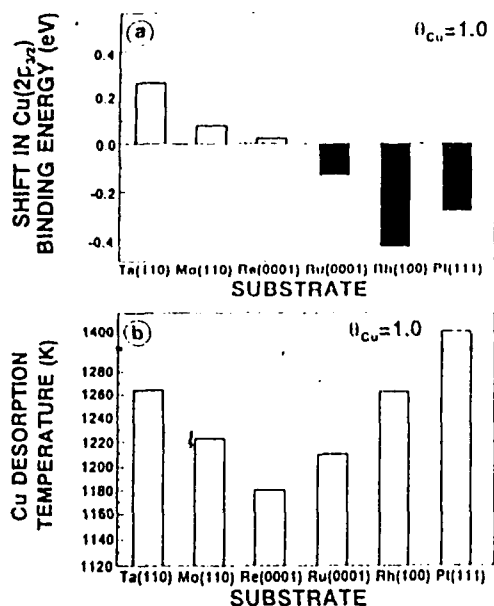
Figure 11. (a) Shift in the Cu(2p$_{3/2}$) binding energy for Cu monolayers supported on Ta(110), Mo(110),[43] Re(0001),[16] Ru(0001),[10] Rh(100),[10] and Pt(111)[17] substrates. (b) Changes in the desorption temperature of Cu monolayers on Ta(110), Mo(110),[20] and Re(0001),[15] Ru(0001),[6] Rh(100),[10] and Pt(111)[59] substrates.
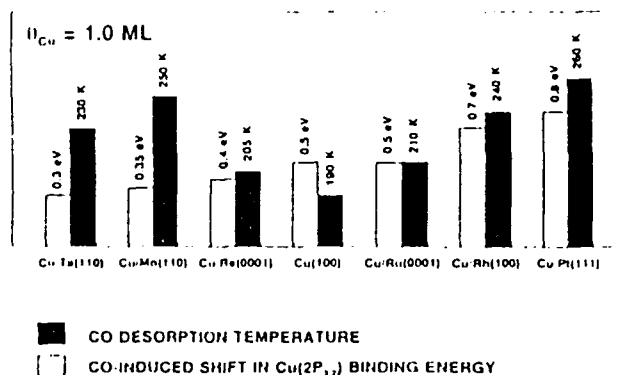

Figure 12. Correlation between the CO desorption temperature and the CO-induced shift in the Cu(2p$_{3/2}$) binding energy for a pseudomorphic Cu monolayer on Ta(110), Mo(110),[43,51] Re(0001),[15,16] Ru(0001),[5,10] Rh(100),[10,11] and Pt(111)[60] substrates and for Cu(100).[29,59]

and have been observed likewise for Ni,[43,49] Pd,[15,43,49] and Ag[50] films on various transition-metal substrates.

Figure 11b shows the desorption temperatures for a monolayer of Cu from several substrates. The higher desorption temperature observed for Cu on Pt(111) likely reflects the alloying that occurs between Cu and Pt. Since the desorption temperature of the Cu overlayer is a good qualitative measure of the bond strength between the Cu and the substrate, this figure indicates that Cu overlayers are bound less tightly to Re than to metals on either end of the transition series. These bond strength differences correlate well with the charge-transfer trends shown in Figure 11a. The greater the magnitude of charge transfer, the greater the bond strength between the overlayer and the substrate. It is important to notice that for certain cases the bond is formed by charge transfer from the Cu overlayer to the substrate and in others by the Cu accepting charge from the substrate. Thus, the data obtained in this study are in excellent agreement with previous data showing that charge transfer between the overlayer and the substrate plays an important role in determining the overlayer–substrate cohesive bond strength. This correlation between the overlayer binding energy shift and the overlayer–substrate bond strength is a general phenomenon and has been observed for Pd and Ni overlayers as discussed elsewhere.[15,49] For a detailed discussion of the relationship between charge transfer and the overlayer–substrate bond, the reader is referred to refs 15, 43, and 49.

Changes in the electronic properties of the overlayer should be reflected in the chemical properties of the surface. Figure 12 is a comparison of the desorption temperatures of CO adsorbed on uniform, annealed, monolayer Cu films and the shift in the Cu(2p$_{3/2}$) binding energy induced by the adsorption of CO. The Cu monolayers which have withdrawn charge from the substrate (shifted toward lower binding energy) show a larger CO-induced shift compared with the Cu monolayers that donated charge to the substrate (shifted toward higher binding energy). The CO-induced shift is always toward higher binding energy, indicating that, when bonded to CO, charge flows from the Cu overlayer. An earlier study of supported Cu overlayers indicated that a good correlation existed between the CO desorption temperature and the CO-induced shift.[49] However, it is noteworthy that the data presented here for Cu/Ta(110) when combined with data for Cu/Mo(110)[43,51] indicate that the CO desorption temperatures

shown in Figure 12, which are proportional to the strength of the Cu–CO bond, do not necessarily correlate with the CO-induced shift (see Figure 12).

The nature of the CO–substrate chemisorptive bond has been the subject of numerous studies, both experimental and theoretical.[52–58] The conventional description of CO chemisorption is based on the Blyholder model[52] where CO–metal bonding is thought to occur via donation of charge from the CO 5σ orbital to an unoccupied metal orbital and by back-donation from the metal d orbitals into the unoccupied 2π orbital of CO. It is generally assumed that as the CO–substrate bond strength increases, the amount of back-donation must also increase. This increase in back-donation into the 2π orbital destabilizes the intermolecular C–O bond and is believed to be a cause of the dissociative adsorption of CO that occurs in very strongly bound CO–metal systems. The increase in CO–Cu binding energy for Cu monolayers on electron-rich substrates has been discussed in detail previously[43,49] and has been attributed to an increase in the ability of the Cu atoms to back-donate charge into the CO 2π orbital, leading to a stronger CO–Cu bond. The increase in CO–Cu binding energy for Cu monolayers on electron-poor substrates, on the other hand, is not consistent with a model where an increase in 2π back-donation leads to an increase in CO–metal bond strength.

Recent theoretical calculations for CO adsorbed on different sized Cu clusters indicate that there are two main contributions to metal–CO bonding: intraspecies charge polarization and interspecies charge transfer.[56,57] The interspecies charge transfer has two main components: CO-σ to metal charge donation and metal to CO-π charge back-donation. Of these, the metal to CO-π back-donation has been shown to be more important in CO–metal bond formation.[54–57] Most previous discussions of CO–metal bonding,[52–54] however, have neglected the importance of the polarization of the metal and CO charge densities to produce an attractive dipole–dipole interaction. The polarization of metal charge away from the CO is a result of the necessity of reducing the repulsive charge superposition interaction between the CO-5σ and metal-s charge distributions during bond formation between Cu and CO. Thus, it is possible that the increase in the CO–Cu bond strength for Cu monolayers on electron-poor substrates could be a direct consequence of the charge transfer from the Cu to the substrate. This would increase the net charge polarization of Cu electron density away from the CO, leading to a stronger dipole–dipole inductive bond between the CO and Cu. Therefore, it appears that the two main factors affecting CO–metal bond strength are (1) the amount of π-back-donation and (2) the polarization interaction between the CO dipole and the partial positive charge on the metal center. The combination of these effects determines the trend seen in Figure 12. The trends shown in Figure 12 should be verifiable through a
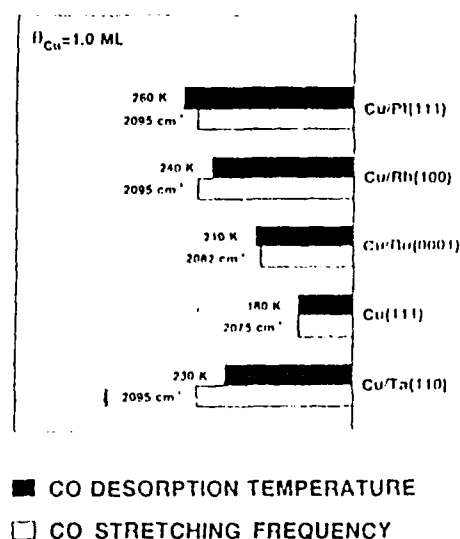
Θ_Cu = 1.0 ML

260 K / 2095 cm⁻¹ — Cu/Pt(111)
240 K / 2095 cm⁻¹ — Cu/Rh(100)
210 K / 2082 cm⁻¹ — Cu/Ru(0001)
180 K / 2075 cm⁻¹ — Cu(111)
230 K / 2095 cm⁻¹ — Cu/Ta(110)

■ CO DESORPTION TEMPERATURE

□ CO STRETCHING FREQUENCY

Figure 13. Correlation between the C–O stretching frequency and the CO desorption temperature for a pseudomorphic Cu monolayer on Ta(110), Ru(0001),[5,8] Rh(100),[11,12] and Pt(111)[17,18] substrates and for Cu(111).[29,30]

comparison of the shifts in the IR stretching frequency of the adsorbed CO.

The stretching frequency of CO adsorbed on a well-ordered Cu monolayer on Ta(110) is 2095 cm⁻¹ as can be seen in Figure 7b. An identical frequency has been observed previously for Cu/Rh(100) and Cu/Pt(111).[12,18] This frequency, however, is quite different from the 2075-cm⁻¹ value observed for CO on Cu(111).[30] In Figure 13, the stretching frequencies and desorption temperatures of CO adsorbed on several monolayer Cu films are compared. From this figure, it is apparent that the stretching frequency of the CO adsorbed on these Cu films correlates well with the CO desorption temperature. The fact that there is a correlation between the CO stretching frequency (which is proportional to the strength of the C–O bond) and the CO desorption temperature (which is proportional to the strength of the Cu–CO bond) is surprising since Figure 12 shows that the CO desorption temperature does not correlate with the CO-induced shift in the Cu($2p_{3/2}$) binding energy (which is proportional to the amount of π-back-donation).

The typical view of the CO–substrate interaction is that an increase in π-back-donation should cause a decrease in the C–O stretching frequency.[52-56] However, it is clear from Figures 12 and 13 that the stretching frequency of CO adsorbed on supported Cu monolayers does *not* correlate with the amount of π-back-donation (as measured by the CO-induced shift). A correlation between the CO stretching frequency (C–O bond strength) and the CO desorption temperature (Cu–CO bond strength) was observed previously for a limited number of supported Cu overlayers[18] and is found to still be valid for the additional data presented in this work. However, this correlation is difficult to explain using simple molecular orbital theory models. Previous calculations have indicated that the CO stretching frequency is influenced by the following: (1) π-back-donation, (2) the interaction of the CO dipole and the electronic charge distribution around the metal atom, and (3) the repulsion occurring when the CO molecule stretches in the presence of a rigid surface (the "wall effect").[33,56,58] Overall, π-back-donation dominates (in agreement with theory[56-58]) and gives rise to a vibrational frequency lower than that of gas-phase CO (2143 cm⁻¹). However, the data shown in Figure 13 imply that the CO stretching frequency is also influenced by the polarization interaction between the CO dipole and the charge density on the metal center. A tighter Cu–CO bond implies a shorter Cu–CO bond length, and a shorter Cu–CO bond length would yield a greater repulsive interaction between the CO dipole and the charge density on the

metal center. This would in turn lead to an increase in the observed CO stretching frequency. It is the complex combination of all of these effects that determines the trend seen in Figure 13. It should be noted that the two main features apparently affecting the CO stretching frequency (π-back-donation and polarization interaction) are the same factors discussed earlier that apparently dominate the CO–Cu bond strength. Additional studies with other metal overlayers need to be conducted to determine whether the effects observed here only occur for Cu films or whether they can be generalized to other overlayer systems.

The IR data for CO/Cu/Ta(110) typically exhibit one adsorption peak for a given Cu coverage. In addition, this feature corresponds to CO adsorbed on a-top sites on the Cu overlayer atoms. In all Cu overlayer systems studied to date, CO adsorption has only been observed to occur on a-top sites.[8,9,12,18] Figure 8 shows that an annealed 1.5-ML Cu film exhibits two features corresponding to CO adsorption on two dissimilar Cu sites. As the CO coverage increases, the low-frequency feature shifts toward higher frequency and at saturation coverage is a barely perceptive shoulder on the main peak at 2102 cm⁻¹. A comparison of parts a and b of Figure 8 implies that the low-frequency feature in Figure 8b is likely due to CO adsorption on the 2-D uniform film and that the high-frequency peak thus likely corresponds to adsorption on Cu clusters on the uniform film. The structure of this overlayer (as discussed earlier) is best described as a 1.2-ML uniform Cu layer with the remaining 0.3 ML existing as clusters on top of this layer. Therefore, the CO on the uniform layer should comprise a larger portion of the total CO surface coverage than the CO on the clusters. However, the reverse is seen in the observed IR spectra and can be attributed to screening and/or sharing of the low-frequency peak (uniform layer) intensity by the high-frequency peak (cluster).[18,33-35] This peak assignment is supported by a comparison of the TPD data in Figure 5b and the spectra in Figure 10b. TPD shows that CO desorbs from the Cu clusters at a lower temperature than from the uniform Cu film. In Figure 10b, the high-frequency feature has been greatly reduced in intensity at 180 K with the low-frequency peak becoming visible. Although the low-frequency feature never becomes the dominant feature, the fact that it becomes visible indicates that the high-frequency peak has been reduced to ≤10% of the total surface CO with intensity sharing perturbing the peak heights to give the observed intensities.[18,33-35]

V. Summary and Conclusions

In this study of ultrathin Cu overlayers on Ta(110) it has again been shown that the properties of a Cu monolayer supported on a dissimilar single-crystal substrate are quite different from those of single-crystal Cu. The differences are reflected as changes in the structural, electronic, and chemisorptive properties of the Cu film. In particular, it was observed that (1) a monolayer or less of Cu on the Ta(110) substrate forms a pseudomorphic film, but annealing ≥1.2 ML of Cu on a Ta(110) substrate induces a change in the film morphology that produces a more densely packed uniform 2-D film with a mismatch occurring along the (1̄10) axis of the substrate. (2) The Cu atoms in the overlayer donate charge to the Ta substrate atoms upon bond formation. (3) CO chemisorbed on the uniform 2-D Cu film is bound more tightly than it is on a pure Cu surface. In addition, the adsorption of CO shifts the binding energy of the Cu to higher energy. (4) The stretching frequency of the adsorbed CO is shifted 20 cm⁻¹ higher than for CO adsorbed on Cu(111). (5) The data presented in this study correlate well with data obtained for other Cu overlayer systems. The charge transfer between the Cu overlayer and the substrate was found to follow a model predicting the charge to flow from the electron-rich metal to the electron-poor metal with Cu acting as a metal with a half-filled valence band. In addition, the bond between the CO and the Cu film was found to be comprised of both π-back-donation and polarization interaction

components. Contributions from both determine the observed bond strength. Finally, it was determined that the stretching frequency of the CO adsorbed on the Cu films correlated with the CO–Cu bond strength, not with the amount of back-donation into the CO 2π orbital.

References and Notes

(1) Rodriguez, J. A.; Goodman, D. W. *J. Phys. Chem.* 1991, 95, 4196 and references therein.

(2) Campbell, C. T. *Annu. Rev. Phys. Chem.* 1990, 41, 775 and references therein.

(3) Kuhn, W. K.; He, J.-W.; Goodman, D. W. *J. Vac. Sci. Technol. A* 1992, 10, 2477.

(4) Christmann, K.; Ertl, G.; Shimizu, H. *J. Catal.* 1980, 61, 397.

(5) Houston, J. E.; Peden, C. H. F.; Blair, D. S.; Goodman, D. W. *Surf. Sci.* 1986, 167, 427.

(6) Yates, J. T.; Peden, C. H. F.; Goodman, D. W. *J. Catal.* 1985, 94, 576.

(7) Houston, J. E.; Peden, C. H. F.; Feibelman, P. J.; Hamann, D. R. *Surf. Sci.* 1987, 192, 457.

(8) Hoffmann, F. M.; Paul, J. *J. Chem. Phys.* 1987, 86, 2990.

(9) Hoffmann, F. M.; Paul, J. *J. Chem. Phys.* 1987, 87, 1857.

(10) Rodriguez, J. A.; Campbell, R. A.; Goodman, D. W. *J. Phys. Chem.* 1991, 95, 2477.

(11) Jiang, X.; Goodman, D. W. *Surf. Sci.* 1991, 255, 1.

(12) He, J.-W.; Kuhn, W. K.; Leung, L.-W. H.; Goodman, D. W. *J. Chem. Phys.* 1990, 93, 7463.

(13) He, J.-W.; Kuhn, W. K.; Goodman, D. W. *J. Phys. Chem.* 1991, 95, 5220.

(14) Ferd, J. S.; Jones, P. D. *Surf. Sci.* 1985, 152/153, 487.

(15) Rodriguez, J. A.; Campbell, R. A.; Goodman, D. W. *J. Vac. Sci. Technol. A* 1992, 10 (4), 2540.

(16) Rodriguez, J. A.; Campbell, R. A.; Goodman, D. W. *Surf. Sci.* 1991, 244, 211.

(17) (a) Shek, M. L.; Stefan, P. M.; Lindau, I.; Spicer, W. E. *Phys. Rev. B* 1983, 27, 7288, 7301. (b) Paffett, M. T.; Campbell, C. T.; Taylor, T. N.; Srinivasan, S. *Surf. Sci.* 1985, 154, 284.

(18) Rodriguez, J. A.; Truong, C. M.; Goodman, D. W. *J. Chem. Phys.* 1992, 96, 7814.

(19) Bauer, E.; Poppa, H. *Thin Solid Films* 1984, 121, 159.

(20) He, J.-W.; Shea, W.-L.; Jiang, X.; Goodman, D. W. *J. Vac. Sci. Technol. A* 1990, 8, 2435.

(21) Bauer, E.; Poppa, H.; Todd, G.; Bonczek, F. *J. Appl. Phys.* 1974, 45, 5164.

(22) Hamadeh, I.; Gomer, R. *Surf. Sci.* 1985, 154, 168.

(23) Lilienkamp, G.; Koziol, C.; Bauer, E. *Surf. Sci.* 1990, 226, 358.

(24) El-Batanouny, M.; Strongin, M. *Phys. Rev. B* 1983, 27, 7277, 7301.

(25) (a) Tracy, J. C. *J. Chem. Phys.* 1972, 56, 2748. (b) Goodman, D. W.; Peden, C. H. F. *J. Chem. Soc., Faraday Trans. 1* 1987, 83, 1967.

(26) Campbell, R. A.; Goodman, D. W. *Rev. Sci. Instrum.* 1992, 63, 172.

(27) Leung, L.-W. H.; He, J.-W.; Goodman, D. W. *J. Chem. Phys.* 1990, 93, 8328.

(28) *Handbook of Chemistry and Physics,* 67th ed.; CRC: Boca Raton, FL, 1986; p D-44.

(29) Egelhoff, W. F., Jr. *Phys. Rev. B* 1984, 29, 4769.

(30) (a) Pritchard, J. *Surf. Sci.* 1979, 79, 231 and references therein. (b) Raval, R.; Parker, S. F.; Pemble, M. E.; Hollins, P.; Pritchard, J.; Chesters, M. A. *Surf. Sci.* 1988, 203, 353.

(31) Hollins, P.; Pritchard, J. In *Vibrational Spectroscopies of Adsorbates;* Willis, R., Ed.; Springer: Berlin, 1980; Vol. 15.

(32) Hoffmann, F. M. *Surf. Sci. Rep.* 1983, 3, 107.

(33) Ryberg, R. In *Advances in Chemical Physics;* Lawley, K. P., Ed.; Wiley: New York, 1989

(34) Persson, B. N. J.; Rydberg, R. *Phys. Rev. B* 1981, 24, 6954.

(35) Browne, V. M.; Fox, S. G.; Hollins, P. *Catal. Today* 1991, 9, 1.

(36) (a) Taylor, N. J. *Surf. Sci.* 1966, 4, 161. (b) Moss, A. R. L.; Blott, B. H. *Surf. Sci.* 1969, 17, 240.

(37) Tikhov, M.; Stolzenberg, M.; Bauer, E. *Phys. Rev. B* 1987, 36, 8719.

(38) Johnson, B. G.; Berlowitz, P. J.; Bartholomew, C. H.; Goodman, D. W. *Surf. Sci.* 1989, 217, 13.

(39) He, J.-W.; Goodman, D. W.; Naugle, D. G.; Cocke, D. L. *Mater. Lett.* 1990, 10, 250.

(40) Tikhov, M.; Bauer, E. *Surf. Sci.* 1990, 232, 73.

(41) He, J.-W.; Goodman, D. W. *Surf. Sci.* 1991, 245, 29.

(42) El-Batanouny, M.; Strongin, M. *Phys. Rev. B* 1985, 95, 4798.

(43) Rodriguez, J. A.; Campbell, R. A.; Goodman, D. W. *J. Phys. Chem.* 1991, 95, 5716.

(44) Schlenk, W.; Bauer, E. *Surf. Sci.* 1980, 93, 9.

(45) Park, C. *Surf. Sci.* 1988, 203, 395.

(46) Shek, M. L.; Stefan, P. M.; Lindau, I.; Spicer, W. E. *Phys. Rev. B* 1983, 27, 7277.

(47) Ruckman, M. W.; Murgai, V.; Strongin, M. *Phys. Rev. B* 1986, 34, 6759.

(48) Graham, G. W. *J. Vac. Sci. Technol. A* 1986, 4, 760.

(49) Campbell, R. A.; Rodriguez, J. A.; Goodman, D. W. *Phys. Rev. B* 1992, 46, 7077.

(50) Pervan, P.; Milun, M. *Surf. Sci.* 1992, 264, 135.

(51) He, J.-W.; Kuhn, W. K.; Goodman, D. W. *Chem. Phys. Lett.* 1991, 177, 109.

(52) Blyholder, G. *J. Phys. Chem.* 1964, 68, 2772.

(53) Heskett, D.; Plummer, E. W.; Messmer, R. P. *Surf. Sci.* 1984, 139, 558.

(54) Kao, C. M.; Messmer, R. P. *Phys. Rev. B* 1985, 31, 4835.

(55) Bagus, P. S.; Hermann, K.; Bauschlicher, Jr., C. W. *J. Chem. Phys.* 1984, 81, 1966.

(56) Muller, P. S.; Bagus, P. S. *J. Vac. Sci. Technol. A* 1985, 3, 1623.

(57) Hermann, K.; Bagus, P. S.; Nelin, C. J. *Phys. Rev. B* 1987, 35, 9467.

(58) Bagus, P. S.; Muller, W. *Chem. Phys. Lett.* 1985, 115, 540.

(59) Gregg, T. W. Unpublished results.

(60) Dubois, L. H.; Zegarski, B. R.; Luftman, H. S. *J. Chem. Phys.* 1987, 87, 1367.

Registry No. Cu, 7440-50-8; Ta, 7440-25-7; CO, 630-08-0.